Chapter 6: Identifying green valley galaxies

This work was done in collaboration with Jinfu Dai for his senior thesis "Exploring the green valley."

6.1 Introduction

The enrichment of the interstellar medium (ISM) and circumgalactic medium (CGM) of a galaxy involves many complicated astrophysical processes, the interplay of which is not yet well understood. A critical problem in galaxy formation is to understand how galaxies transition from the blue sequence to the red cloud of the optical color-magnitude diagram. Star formation is thought to be quenching in galaxies moving through the green valley, but the relevant baryonic processes (gas cooling, feedback, etc.) are very complex and heavily interdependent. Investigating the star formation history and chemical evolution of galaxies in the green valley should provide clues as to the evolution of a galaxy through the color-magnitude diagram.

Large galaxy surveys (like the Sloan Digital Sky Survey; York et al., 2000) revealed the structure of the color-magnitude diagram (CMD). As seen in Fig. 6.1, the $u - r$ CMD is dominated by two major subgroups of galaxies: the red cloud and the blue sequence (Strateva et al., 2001; Baldry et al., 2004). Most galaxies that reside in the red cloud appear to be older, elliptical galaxies that are no longer making stars ("red and dead"). On the other hand, the blue sequence consists of mostly spiral and irregular galaxies which are actively forming stars.

There are a number of different astrophysical processes which simultaneously evolve a galaxy's stellar and gas content. AGN feedback strongly affects massive galaxies, while dwarf galaxy feedback is dominated by supernovae. Both AGN and supernovae can inject enough energy into a galaxy's ISM to prevent its cooling, thereby quenching star formation. In addition to internal mechanisms, galaxies will often experience interactions in denser environmental regions. Depending on the properties of the galaxies involved (mass, speed, etc.), these interactions can either strip gas from the galaxy (removing a primary source of fuel for future star formation), or they can trigger a burst of star

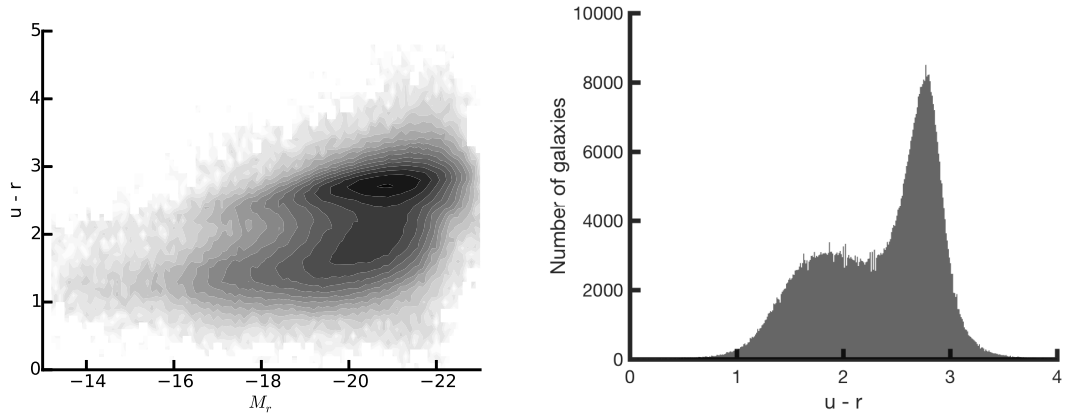

Figure 6.1: The optical color-magnitude diagram (left) and histogram of $u - r$ colors (right) of galaxies in SDSS DR7. There are two groups of galaxies, the populations of which are well fit by the sum of two Gaussians. They are aptly named the "red cloud" and the "blue sequence."

formation.

Our current theory of galactic evolution necessitates the existence of a transition period in a galaxy's lifetime, when the galaxy migrates from the star-forming blue sequence to the red cloud on the optical CMD. However, the $u - r$ CMD is very well fit by the sum of only two Gaussians (Strateva et al., 2001; Baldry et al., 2004); an intermediate population is not present in the optical CMD. Early explanations developed to reconcile this apparent discrepancy between theory and observation included a sudden transition from the blue sequence to the red cloud, often associated with some star-formation quenching mechanism.

Dubbed the "green valley," it is thought that star formation is being quenched in the galaxies moving through the green valley (Martin et al., 2007). So far, results of studies done with these green valley galaxies have been inconclusive as to why or how this is occurs.

6.2 Calculating the color of a galaxy

A galaxy's color is the ratio of the flux emitted by the galaxy in two different bands. The stellar population of a galaxy will determine its color — redder galaxies contain much older, cooler stars, while the spectrum of a bluer galaxy is produced by light from much younger, hotter stars. A galaxy's color is independent of its redshift, so only photometry is needed to calculate the ratio.

While the KIAS-VAGC catalog (described below in Section 6.3.1) provides the $u - r$ color for all galaxies in SDSS, we make use of the Petrosian fluxes in the NSA (described in Section 6.3.2) to calculate the UV–optical color. The NUV$-r$ color is calculated by

$$\mathrm{NUV} - r = -2.5 \log \left(\frac{f_{NUV}}{f_r} \right) \tag{6.1}$$

where f_{NUV} is the Petrosian flux in the NUV-band of GALEX, and f_r is the Petrosian flux in the r-band of SDSS.

6.3 SDSS and GALEX data

We use the photometric data from SDSS (optical) and GALEX (ultraviolet) as cross-matched in the NSA.

6.3.1 Optical data — SDSS

The SDSS Data Release 7 (Abazajian et al., 2009, DR7) is a wide-field multi-band imaging and spectroscopic survey that uses drift scanning to map approximately one-quarter of the northern sky. A dedicated 2.5-meter telescope at the Apache Point Observatory in New Mexico takes photometric data in the five-band SDSS system — u, g, r, i, and z (Fukugita et al., 1996; Gunn et al., 1998). Galaxies with a Petrosian r-band apparent magnitude $m_r < 17.77$ are selected for spectroscopic analysis (Lupton et al., 2001; Strauss et al., 2002). Gas-phase chemical abundances are calculated via the Direct T_e method using emission-line fluxes measured by the MPA-JHU catalog[1] and published in Douglass & Vogeley (2017, in prep). The large-scale environment of the galaxies is based on the void catalog compiled by Pan et al. (2012). This void catalog is constructed from SDSS DR7 using the VoidFinder algorithm of Hoyle & Vogeley (2002). Galaxies which are located within the identified voids are labeled as void galaxies; those which do not reside in a void are designated as wall galaxies. Because the minimum diameter of a void is defined as 10 h^{-1}Mpc, the large-scale environment of galaxies within 5 h^{-1}Mpc of the edge of the SDSS DR7 footprint cannot be described, so their environment is labeled as unknown.

[1] Available at `http://www.mpa-garching.mpg.de/SDSS/DR7`

The Korea Institute for Advanced Study Value-Added Galaxy Catalog (Choi et al., 2010, KIAS-VAGC) contains galaxies from the SDSS DR7 main sky survey based on the New York University Value-Added Galaxy Catalog Data Release 7 (Blanton et al., 2005, NYU-VAGC). It provides a morphological class and type following the automated morphology classification scheme of Park & Choi (2005), using the color $u-r$, color gradient $\Delta(g-r)$, and inverse concentration index. We use the absolute magnitudes as listed in the KIAS-VAGC.

6.3.2 UV data — GALEX

The Galaxy Evolution Explorer (Martin et al., 2005, GALEX) is an orbiting space telescope conducting an extra-galactic ultraviolet all-sky survey. The instrument allows imaging and spectroscopic observations in two ultraviolet bands — Far UV (FUV, 1350–1780Å) and Near UV (NUV, 1770–2730Å) (Morrissey et al., 2007). The NUV-r colors used in this study are calculated from the azimuthally-averaged SDSS-style Petrosian fluxes provided in the NASA-Sloan Atlas version 0.1.2 (Blanton et al., 2011, NSA).

6.4 Classification of galaxies in the color-magnitude diagram

Combining the results of GALEX with the optical photometry of SDSS, we construct a NUV$-r$ CMD. Probing light from even younger stars in the galaxies, GALEX is able to increase the separation of the blue sequence and red cloud populations of the optical CMD, revealing a third, smaller population of galaxies (Wyder et al., 2007).

This analysis reveals a population of galaxies that lie in the Green Valley on the NUV$-r$ color-magnitude diagram, identified independent of their location on the diagram. Rather than being classified based on arbitrary limits placed on the NUV$-r$ values (as done by Schawinski et al., 2014; Salim, 2014), the galaxies can be easily separated into three distinct populations based on the galaxies' morphological types as calculated in the KIAS-VAGC; this can be seen in Fig. 6.2. Defined by the $u-r$ color and the color gradient $\Delta(g-i)$, it is novel that an estimate of the morphological type of the galaxies is an adequate classification for the three populations of the NUV$-r$ CMD. In addition, Fig. 6.3 shows a histogram of the galaxies which overlap in both

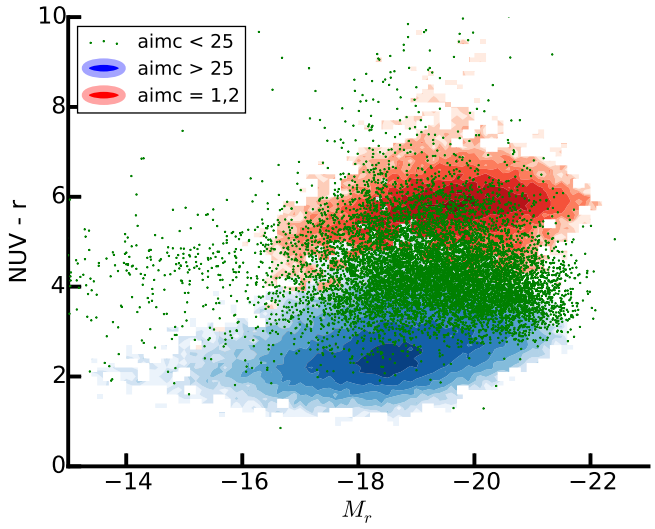

Figure 6.2: The NUV$-r$ color-magnitude diagram of galaxies in SDSS DR7. Those galaxies in the red contours have morphological classifications of either normal early types (aimc = 1) or blue early types (aimc = 2), as determined by the KIAS-VAGC. The green points represent a subset of the normal late type galaxies (aimc less than 25, excluding those with values of 1 or 2), and the blue contours represents the remaining normal late type galaxies (aimc greater than 25). It is clear that this morphological classification defines those galaxies that are transitioning from the blue sequence to the red cloud.

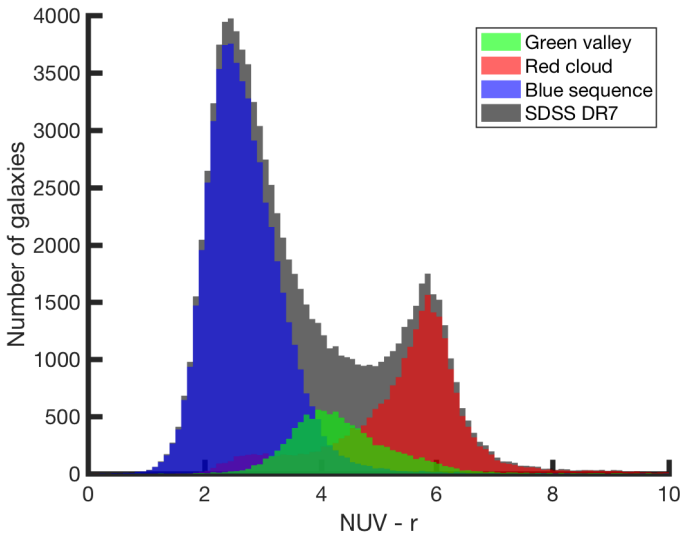

Figure 6.3: A histogram of the NUV$-r$ color of those SDSS DR7 galaxies which are also detected in GALEX. The red cloud, blue sequence, and green valley populations are separated by the morphological types as defined by the KIAS-VAGC. It is readily apparent that the green valley galaxies exist in the space between the red cloud and blue sequence.

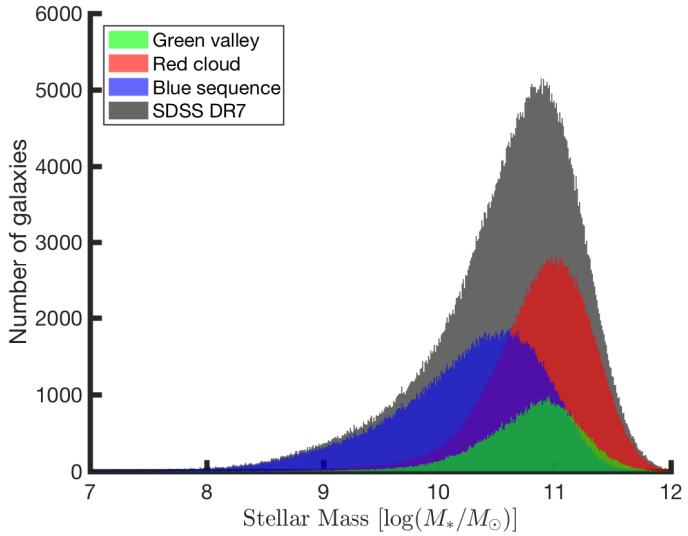

Figure 6.4: The distribution of stellar mass for all galaxies in SDSS DR7, separated by their morphological type. The galaxies in the green valley have stellar masses comparable to those in the red cloud. The stellar masses of those galaxies in the blue sequence range from the lowest mass objects up through the stellar masses of the green valley galaxies.

GALEX and SDSS, separated by their morphological classification from the KIAS-VAGC. It shows that the three populations are well fit by three Gaussians — the new population in the middle is the transient galaxy population originally "missing" from the optical CMD.

The morphological classification that we use to isolate the green valley population is relatively unique in that it is analytic; morphological classification attempts are often completed in a more subjective manner (such as the GalaxyZoo, Lintott et al., 2011). In particular, the morphological type provided in KIAS-VAGC is a combination of the color $u-r$ and the color gradient $\Delta(g-i)$. Both these quantities are independent of the NUV$-r$ CMD, which is part of the novelty behind why this measure separates the galaxies into the three evolutionary stages of the CMD so well.

6.4.1 Properties of the Green Valley Galaxies

Stellar mass

If the green valley galaxies represent those galaxies transitioning between the blue sequence and red cloud, then their stellar masses should overlap the masses in both these populations. The distribution of the stellar masses for the galaxies in SDSS DR7 is shown in Fig. 6.4. We can see

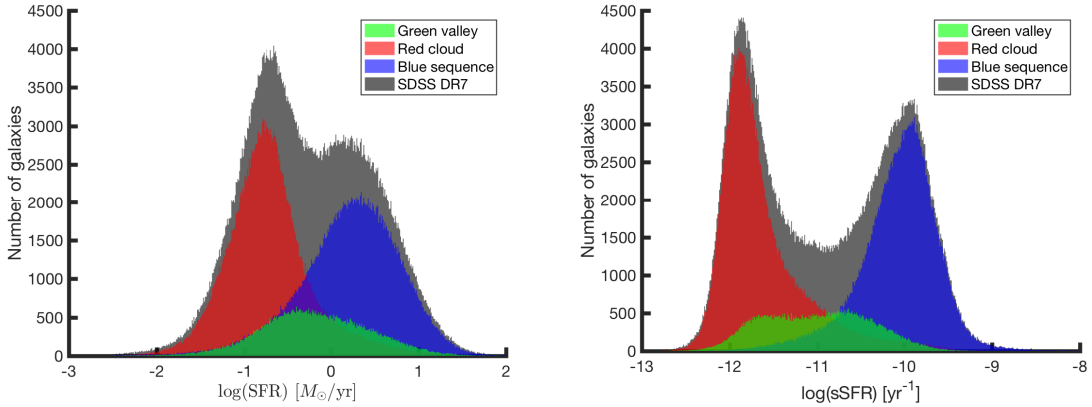

Figure 6.5: The distribution of SFR (left panel) and sSFR (right panel) for all galaxies in SDSS DR7, separated by their morphological type. The green valley galaxies occupy the intermediate SFRs, while galaxies in the red cloud have low SFRs and galaxies in the blue sequence have higher SFRs. The same ranges exist for the sSFRs, although the green valley galaxies extend well into the range of sSFRs occupied by the galaxies in the red cloud.

that the galaxies in the green valley have stellar masses comparable to those in the red cloud. The stellar masses of those galaxies in the blue sequence range from the lowest mass objects up through the stellar masses of the green valley galaxies. The distribution of stellar masses of blue sequence galaxies should be much broader than the range of masses seen in the red cloud galaxies, since those in the blue sequence are slowly building up their stellar mass by forming stars from both their gas reservoirs and cool gas falling onto the galaxy. Galaxies in the red cloud are fairly stagnant in their star formation, so the range of stellar masses of these galaxies will be more narrow than that of the blue sequence. If the green valley galaxies are transitioning between the two populations due to a quenching of star formation or a sudden burst of star formation, then we would expect their mass range to cover the high-mass end of the blue sequence and most of the red cloud. These expectations are met in Fig. 6.4.

Star formation rates

If green valley galaxies are transitioning between the blue sequence and red cloud, then they should have intermediate (s)SFRs. The distribution of SFR and sSFR for the galaxies in SDSS DR7 are shown in Fig. 6.5, with the galaxies separated by their morphological types. We see that the distribution of SFRs for galaxies in the green valley peaks around log(SFR) ~ -0.5, in between the

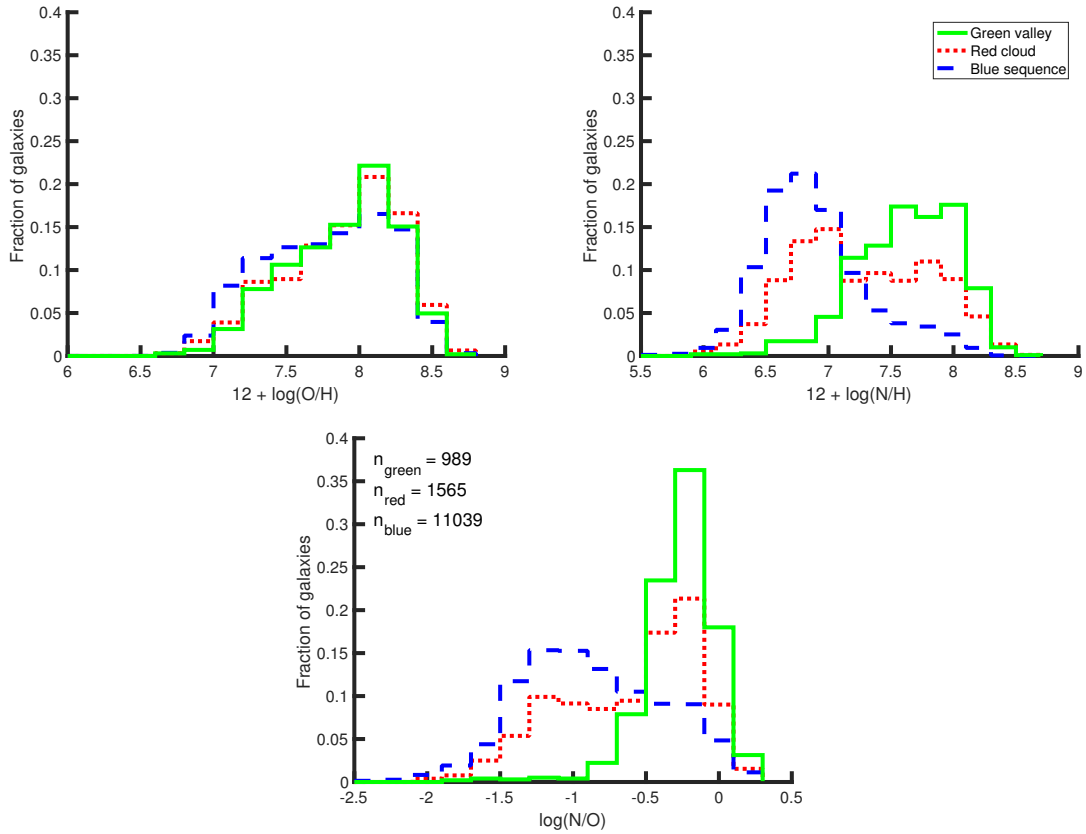

Figure 6.6: Histograms of the oxygen abundance (top left), nitrogen abundance (top right), and N/O ratio (bottom center) of the cross-matched SDSS DR7 – GALEX galaxies, separated into their locations on the NUV$-r$ color-magnitude diagram according to the morphological type listed in the KIAS-VAGC. It is readily apparent that the green valley galaxies have higher nitrogen abundances than those in the blue sequence (and some of the red cloud). This, therefore, corresponds to them having high N/O ratios.

ranges occupied by the red cloud and blue sequence galaxies. A similar distribution is shown for the sSFRs, although the green valley galaxies extend well into the range of sSFRs occupied by the galaxies in the red cloud. Salim (2014) describes transitional galaxies (those in the green valley) to have lower sSFRs than galaxies in the blue sequence, specifically $-11.8 < \log(\text{sSFR}) < -10.8$. While our results do indicate that green valley galaxies have lower sSFRs than those in the blue sequence, we find that their range of sSFR is almost double the width of that described in Salim (2014). The green valley galaxies have a sSFR within the range $-12 \lesssim \log(\text{sSFR}) \lesssim -10$.

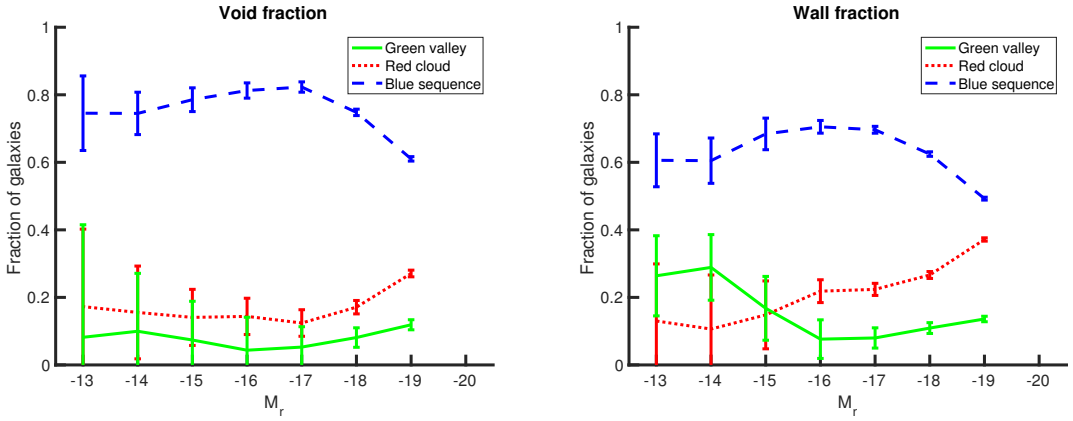

Figure 6.7: Fraction of void (left) and wall (right) galaxies in each of the three CMD populations, classified by the morphological type listed in the KIAS-VAGC. There is a higher fraction of green valley dwarf galaxies ($M_r > -17$) found in the more dense environments than in the voids. This would indicate that void galaxies are slightly behind wall galaxies in their evolution, matching predictions based on the ΛCDM cosmology.

Gas-phase chemical abundances

Estimates of the gas-phase chemical abundances of galaxies probe their integrated star formation histories, which can provide insight into the enrichment of the ISM and CGM. A few of the galaxies for which Douglass & Vogeley (2017, in prep) are able to estimate metallicities reside in the green valley. When compared with the metallicities of galaxies in the blue sequence and red cloud, Fig. 6.6 shows that the green valley galaxies have higher nitrogen abundances than star-forming galaxies in the blue sequence (and some of the red cloud). With oxygen abundances that fall within the same range as the other two galaxy populations, this shift causes the N/O ratio to be much higher in green valley galaxies than in the blue sequence.

Large-scale environment

When we separate the galaxies in each of the three populations by their large-scale environment, we discover a variation in these populations as a function of luminosity. As we see in Fig. 6.7, the fraction of galaxies in the green valley depends on the large-scale environment, even at fixed stellar mass or luminosity. A larger fraction of faint wall galaxies are found in the green valley than for faint void galaxies.

6.5 Understanding green valley galaxies

Galaxies in the green valley are described to be in a transitional period of the galaxy's life cycle, where they are being quenched in their star formation or are beginning to form stars after being quiescent. Here, we are able to quantitatively define galaxies in the green valley of the UV-optical CMD. We find them to be of comparable stellar mass to galaxies in the red cloud, have intermediate SFRs and intermediate-to-low sSFRs, and have higher gas-phase nitrogen abundances and N/O ratios than galaxies in the blue sequence.

The range of stellar masses in galaxies from the green valley in Fig. 6.4 shows us that these galaxies have completed most of their star formation. They have acquired enough stars to have converted much of their gas into heavier elements. Combined with the intermediate SFRs and intermediate-to-low sSFRs seen in Fig. 6.5, this tells us that these galaxies are no longer forming stars at a high rate. This is most likely due to an extinction of available cool gas from which to form stars. These galaxies are reaching a natural point in their evolution where they transition from an active star formation period to a quieter, more quiescent lifestyle.

As explained in Douglass & Vogeley (2017b), nitrogen is thought to be produced in both a primary and secondary stage, depending on the presence of other heavy elements. The fact that the galaxies in the green valley have higher nitrogen abundances compared to those in the blue sequence indicate that they are building up a surplus of nitrogen, most likely due to the presence of heavier elements at the later star formation episodes. The surplus of heavier elements allows the CNO cycle to commence earlier in the stars' lifetimes, producing nitrogen at a higher rate than oxygen. It is also possible that the higher nitrogen abundances are a sign that the galaxies' intermediate mass stars (those primarily responsible for nitrogen synthesis) have expired. This surplus of nitrogen results in the high N/O ratios seen for the green valley galaxies in Fig. 6.6.

Fig. 6.7 shows a higher fraction of faint wall galaxies than faint void galaxies are in the green valley. This would indicate that void galaxies are slightly behind wall galaxies in their evolution, matching predictions based on the ΛCDM cosmology. These results also coincide with the observations of Douglass & Vogeley (2017b) and Douglass & Vogeley (2017, in prep). They find that, for

dwarf galaxies ($M_r > -17$), those which exist in voids may have commenced their star formation at a later time and have not experienced the same cosmic downsizing as dwarf galaxies residing in denser regions. The higher fraction of wall dwarf galaxies in the green valley might also point to an environmental influence on the reason for transitioning through the green valley, such as ram pressure stripping, which would occur much less frequently in the void environment. However, the existence of void galaxies in the green valley indicate that galaxy interactions cannot be the only star formation quenching mechanism.

6.5.1 Gas content indicators

If a galaxy's star formation is quenched due to a loss of cold gas, then its HI content will be lower than other galaxies of a similar stellar mass and large-scale environment. Schawinski et al. (2014) finds that 48% of the late-type galaxies they define to be in the green valley have H I detections in the ALFALFA survey, consistent with a high probability of gas resevoir retention. Likewise, Catinella et al. (2012) shows that the gas fraction (M_{HI}/M_*) correlates with the NUV$-r$ color, suggesting that the transition of galaxies into the green valley is not due to an abrupt change in the galaxy's neutral gas supply. If it is quenched due to a high gas temperature (from AGN or supernovae feedback), then the temperature of the gas will be higher than others of a similar size. These factors will also help to determine when and why a galaxy transitions from star-forming to quiescent (and maybe back to star-forming).

6.5.2 Evidence of AGN feedback

To understand the gas-phase chemical abundances of the green valley galaxies, we compare Fig. 6.6 with the distribution of the gas-phase chemical abundances of star-forming and composite galaxies and galaxies with an AGN shown in Fig. 6.8. We see that the galaxies with an AGN have the most similar distributions in the three abundance ratios as the green valley galaxies: both groups have similar oxygen abundances (O/H) and higher nitrogen abundances (N/H) and N/O ratios than the star-forming galaxies. This might indicate a link between green valley galaxies and a host AGN. The presence of an AGN in green valley galaxies would support other studies of the transition of

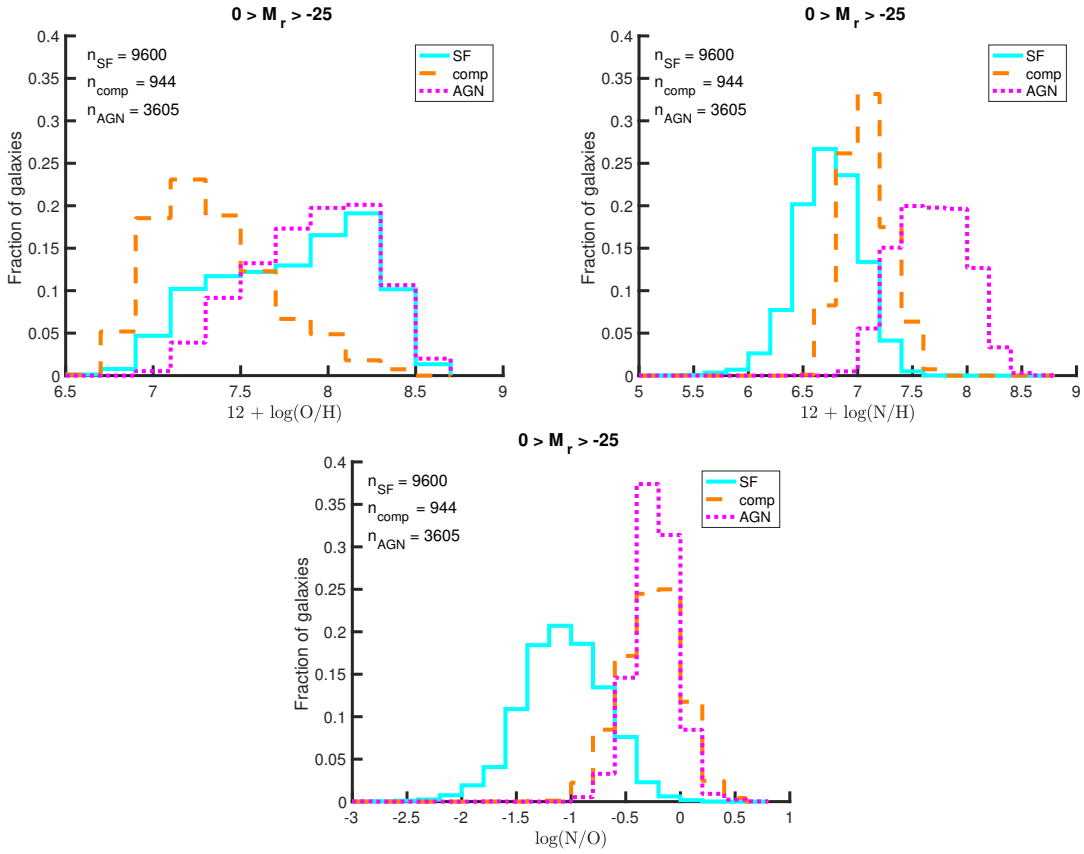

Figure 6.8: Distribution of the gas-phase oxygen abundance (O/H, top left), nitrogen abundance (N/H, top right), and N/O ratio (bottom center) of the SDSS DR7 galaxies with detectable emission lines for abundance calculations with the Direct T_e method. Star-forming galaxies are shown with a solid cyan line, while composite galaxies are a dashed orange line and galaxies with an AGN are represented as a dotted magenta line. Composite galaxies have lower oxygen abundances than both star-forming galaxies and those with an AGN. The nitrogen abundance range is different for each of the three classes, with star-forming galaxies having the lowest nitrogen abundances, AGN having the highest, and composite galaxies in the middle. Therefore, star-forming galaxies have N/O ratios < 0, while composite galaxies and galaxies with an AGN have N/O ratios between -1 and 0.5.

galaxies from the blue sequence to the red cloud, which attribute the quenching of star formation to accretion of a central black hole (e.g., Croton et al., 2006; Stasińska et al., 2008).

6.6 Conclusions

We can define galaxies which are transitioning through the green valley of the color-magnitude diagram by combining the galaxy's color, color gradient, and inverse concentration index. Galaxies with a magnitude less than 25 for the morphological type as calculated in the KIAS-VAGC exist in the green valley portion of the UV-optical color magnitude diagram. Galaxies defined as early types (morphological type values equal to 1 or 2) are in the red cloud, while those with morphological type values greater than 25 are in the blue sequence. With this quantitative definition for galaxies transitioning through the green valley, we can begin to understand the properties of green valley galaxies and the evolution of galaxies.

Based on our analysis, green valley galaxies have stellar masses comparable to those in the red cloud. They have intermediate SFRs, and low-to-intermediate sSFRs. Green valley galaxies also have high gas-phase nitrogen abundances (N/H), resulting in high N/O ratios. While their SFRs show that something has quenched their star formation, their stellar masses inform us that this is not due to any premature quenching mechanism. The high nitrogen abundances in the green valley galaxies indicate that the galaxies are either no longer forming stars (since nitrogen is produced in lower mass stars than oxygen), or that the galaxies were able to produce both primary and secondary nitrogen (heavy elements were present during the last few star formation episodes to permit the CNO cycle to commence earlier). This chemical abundance pattern (normal oxygen, high nitrogen, and high N/O ratio) is also seen in galaxies classified as AGN, indicating that the galaxies in the green valley have an AGN.

There is a higher fraction of faint wall galaxies than faint void galaxies in the green valley. In conjunction with the conclusions of Douglass & Vogeley (2017b) and Douglass & Vogeley (2017, in prep), this indicates that void dwarf galaxies are less evolved than dwarf galaxies in denser environments. It would be beneficial to investigate the small-scale ($\sim 1\ h^{-1}$Mpc) environment of galaxies in the green valley, to determine if any interactions are responsible for the transitional state.

Bibliography

Abazajian, K. N., Adelman-McCarthy, J., Agueros, M. A., et al. 2009, ApJS, 182, 543

Ahn, C. P., Alexandroff, R., Allende Prieto, C., et al. 2012, ApJS, 203, 21

Amorín, R. O., Pérez-Montero, E., & Vílchez, J. M. 2010, ApJL, 715, L128

Andrews, B. H., & Martini, P. 2013, ApJ, 765, 140

Ann, H. B., Park, C., & Choi, Y.-Y. 2008, MNRAS, 389, 86

Asplund, M., Grevesse, N., Sauval, A. J., & Scott, P. 2009, ARA&A, 47, 481

Baldry, I. K., Glazebrook, K., Brinkmann, J., et al. 2004, ApJ, 600, 681

Bell, E. F., & de Jong, R. S. 2000, MNRAS, 312, 497

Berg, D. A., Skillman, E. D., Marble, A. R., et al. 2012, ApJ, 754, 98

Berlind, A. A., Frieman, J., Weinberg, D. H., et al. 2006, ApJS, 167, 1

Beygu, B., Kreckel, K., van der Hulst, J. M., et al. 2016, MNRAS, 458, 394

Beygu, B., Peletier, R. F., Hulst, J. M. v. d., et al. 2017, MNRAS, 464, 666

Blanton, M. R., Kazin, E., Muna, D., Weaver, B. A., & Price-Whelan, A. 2011, AJ, 142, 31

Blanton, M. R., Lin, H., Lupton, R. H., et al. 2003, AJ, 125, 2276

Blanton, M. R., Schlegel, D. J., Strauss, M. A., et al. 2005, AJ, 129, 2562

Bond, J. R., Kofman, L., & Pogosyan, D. 1996, Nature, 380, 603

Brinchmann, J., Charlot, S., White, S. D. M., et al. 2004, MNRAS, 351, 1151

Brisbin, D., & Harwit, M. 2012, ApJ, 750, 142

Catinella, B., Schiminovich, D., Kauffmann, G., et al. 2012, A&A, 544, A65

Cen, R. 2011, ApJ, 741, 99

Choi, Y.-Y., Han, D.-H., & Kim, S. S. 2010, JKAS, 43, 191

Contini, T., Treyer, M. A., Sullivan, M., & Ellis, R. S. 2002, MNRAS, 330, 75

Cooper, M. C., Tremonti, C. A., Newman, J. A., & Zabludoff, A. I. 2008, MNRAS, 390, 245

Croton, D. J., Farrar, G. R., Norberg, P., et al. 2005, MNRAS, 356, 1155

Croton, D. J., Springel, V., White, S. D. M., et al. 2006, MNRAS, 365, 11

Cybulski, R., Yun, M. S., Fazio, G. G., & Gutermuth, R. A. 2014, MNRAS, 439, 3564

de Lapparent, V., Geller, M. J., & Huchra, J. P. 1986, ApJL, 302, L1

De Robertis, M., Dufour, R., & Hunt, R. 1987, JRASC, 81, 195

Deng, X.-F. 2011, AJ, 141, 162

Dopita, M. A., Sutherland, R. S., Nicholls, D. C., Kewley, L. J., & Vogt, F. P. A. 2013, ApJS, 208, 10

Douglass, K. A., & Vogeley, M. S. 2017a, ApJ, 834, 186

—. 2017b, ApJ, 837, 42

Dressler, A. 1980, ApJ, 236, 351

Ellison, S. L., Simard, L., Cowan, N. B., et al. 2009, MNRAS, 396, 1257

Fakhouri, O., & Ma, C.-P. 2009, MNRAS, 394, 1825

Filho, M. E., Sánchez Almeida, J., Muñoz-Tuñón, C., et al. 2015, ApJ, 802, 82

Fukugita, M., Ichikawa, T., Gunn, J. E., et al. 1996, AJ, 111, 1748

Gao, L., & White, S. D. M. 2007, MNRAS, 377, L5

Garnett, D. R. 1992, AJ, 103, 1330

Geha, M., Blanton, M. R., Yan, R., & Tinker, J. L. 2012, ApJ, 757, 85

Goldberg, D. M., Jones, T. D., Hoyle, F., et al. 2005, ApJ, 621, 643

Goldberg, D. M., & Vogeley, M. S. 2004, ApJ, 605, 1

Gottlöber, S., Łokas, E. L., Klypin, A., & Hoffman, Y. 2003, MNRAS, 344, 715

Gregory, S. A., & Thompson, L. A. 1978, ApJ, 222, 784

Grogin, N. A., & Geller, M. J. 1999, AJ, 118, 2561

—. 2000, AJ, 119, 32

Gunn, J. E., Carr, M., Rockosi, C., et al. 1998, AJ, 116, 3040

Guseva, N., Papaderos, P., Meyer, H., Izotov, Y., & Fricke, K. 2009, A&A, 505, 63

Henry, A., Martin, C. L., Finlator, K., & Dressler, A. 2013, ApJ, 769, 148

Henry, R. B. C., Edmunds, M. G., & Köppen, J. 2000, ApJ, 541, 660

Henry, R. B. C., Nava, A., & Prochaska, J. X. 2006, ApJ, 647, 984

Hirschmann, M., De Lucia, G., Wilman, D., et al. 2014, MNRAS, 444, 2938

Hoversten, E. A., & Glazebrook, K. 2008, ApJ, 675, 163

Hoyle, F., Rojas, R. R., Vogeley, M. S., & Brinkmann, J. 2005, ApJ, 620, 618

Hoyle, F., & Vogeley, M. S. 2002, ApJ, 566, 641

Hoyle, F., Vogeley, M. S., & Pan, D. 2012, MNRAS, 426, 3041

Huchra, J. P., & Geller, M. J. 1982, ApJ, 257, 423

Hughes, T. M., Cortese, L., Boselli, A., Gavazzi, G., & Davies, J. I. 2013, A&A, 550, A115

Hwang, H. S., & Park, C. 2010, ApJ, 720, 522

Izotov, Y. I., Stasińska, G., Meynet, G., Guseva, N. G., & Thuan, T. X. 2006, A&A, 448, 955

Izotov, Y. I., & Thuan, T. X. 1999, ApJ, 511, 639

Jones, M. G., Papastergis, E., Haynes, M. P., & Giovanelli, R. 2016, MNRAS, 457, 4393

Jung, I., Lee, J., & Yi, S. K. 2014, ApJ, 794, 74

Kauffmann, G., Heckman, T. M., White, S. D. M., et al. 2003, MNRAS, 341, 33

Kennicutt, Jr., R. C., Bresolin, F., & Garnett, D. R. 2003, ApJ, 591, 801

Kereš, D., Katz, N., Weinberg, D. H., & Davé, R. 2005, MNRAS, 363, 2

Kewley, L. J., & Dopita, M. A. 2002, ApJS, 142, 35

Kewley, L. J., & Ellison, S. L. 2008, ApJ, 681, 1183

Kirshner, R. P., Oemler, Jr., A., Schechter, P. L., & Shectman, S. A. 1981, ApJL, 248, L57

Kniazev, A. Y., Zijlstra, A. A., Grebel, E. K., et al. 2008, MNRAS, 388, 1667

Kravtsov, A. 2009, in Astronomical Society of the Pacific Conference Series, Vol. 419, Galaxy Evolution: Emerging Insights and Future Challenges, ed. S. Jogee, I. Marinova, L. Hao, & G. A. Blanc, 283

Kreckel, K., Croxall, K., Groves, B., van de Weygaert, R., & Pogge, R. W. 2015, ApJL, 798, L15

Kreckel, K., Platen, E., Aragon-Calvo, M., et al. 2012, AJ, 144, 16

Kroupa, P. 2001, MNRAS, 322, 231

—. 2002, Science, 295, 82

Lackner, C. N., Cen, R., Ostriker, J. P., & Joung, M. R. 2012, MNRAS, 425, 641

Lara-Lopez, M., Hopkins, A., Lopez-Sanchez, A., et al. 2013, MNRAS, 434, 451

Lee, J. C., Salzer, J. J., & Melbourne, J. 2004, ApJ, 616, 752

Lintott, C., Schawinski, K., Bamford, S., et al. 2011, MNRAS, 410, 166

Lupton, R., Gunn, J. E., Ivezić, Z., Knapp, G. R., & Kent, S. 2001, in Astronomical Society of the Pacific Conference Series, Vol. 238, Astronomical Data Analysis Software and Systems X, ed. F. R. Harnden, Jr., F. A. Primini, & H. E. Payne, 269

Luridiana, V., Morisset, C., & Shaw, R. A. 2015, A&A, 573, A42

Mannucci, F., Cresci, G., Maiolino, R., Marconi, A., & Gnerucci, A. 2010, MNRAS, 408, 2115

Marino, R. A., Rosales-Ortega, F. F., Sánchez, S. F., et al. 2013, A&A, 559, A114

Martin, D. C., Fanson, J., Schiminovich, D., et al. 2005, ApJ, 619, L1

Martin, D. C., Wyder, T. K., Schiminovich, D., et al. 2007, ApJSS, 173, 342

Matteucci, F. 1986, MNRAS, 221, 911

Meurer, G. R., Wong, O. I., Kim, J. H., et al. 2009, ApJ, 695, 765

Moorman, C. M., Moreno, J., White, A., et al. 2016, ApJ, 831, 118

Moorman, C. M., Vogeley, M. S., Hoyle, F., et al. 2015, ApJ, 810, 108

Moran, S. M., Heckman, T. M., Kauffmann, G., et al. 2012, ApJ, 745, 66

Morrissey, P., Conrow, T., Barlow, T. A., et al. 2007, ApJS, 173, 682

Mouhcine, M., Baldry, I., & Bamford, S. 2007, MNRAS, 382, 801

Muratov, A. L., Kereš, D., Faucher-Giguère, C.-A., et al. 2017, MNRAS, 468, 4170

Nava, A., Casebeer, D., Henry, R. B. C., & Jevremovic, D. 2006, ApJ, 645, 1076

Nicholls, D. C., Dopita, M. A., Sutherland, R. S., et al. 2014a, ApJ, 786, 155

Nicholls, D. C., Jerjen, H., Dopita, M. A., & Basurah, H. 2014b, ApJ, 780, 88

Osterbrock, D. E. 1989, Astrophysics of Gaseous Nebulae and Active Galactic Nuclei (Mill Valley, CA: University Science Books)

Pan, D. C., Vogeley, M. S., Hoyle, F., Choi, Y.-Y., & Park, C. 2012, MNRAS, 421, 926

Park, C., & Choi, Y.-Y. 2005, ApJ, 635, L29

—. 2009, ApJ, 691, 1828

Park, C., Choi, Y.-Y., Vogeley, M. S., et al. 2007, ApJ, 658, 898

Patiri, S. G., Prada, F., Holtzman, J., Klypin, A., & Betancort-Rijo, J. 2006, MNRAS, 372, 1710

Pérez-Montero, E., & Contini, T. 2009, MNRAS, 398, 949

Pérez-Montero, E., Contini, T., Lamareille, F., et al. 2013, A&A, 549, A25

Pettini, M., & Pagel, B. E. 2004, MNRAS, 348, L59

Pilyugin, L. S., Contini, T., & Vílchez, J. M. 2004, A&A, 423, 427

Pilyugin, L. S., & Mattsson, L. 2011, MNRAS, 412, 1145

Pilyugin, L. S., Mollá, M., Ferrini, F., & Vílchez, J. M. 2002, A&A, 383, 14

Pilyugin, L. S., & Thuan, T. X. 2007, ApJ, 669, 299

Pilyugin, L. S., Thuan, T. X., & Vílchez, J. M. 2006, MNRAS, 367, 1139

Pustilnik, S. A. 2014, ArXiv e-prints, 1412.1316

Pustilnik, S. A., Engels, D., Kniazev, A. Y., et al. 2006, AstL, 32, 228

Pustilnik, S. A., Martin, J.-M., Lyamina, Y. A., & Kniazev, A. Y. 2013, MNRAS, 432, 2224

Pustilnik, S. A., Martin, J.-M., Tepliakova, A. L., & Kniazev, A. Y. 2011a, MNRAS, 417, 1335

Pustilnik, S. A., Tepliakova, A. L., & Kniazev, A. Y. 2011b, Astrophysical Bulletin, 66, 255

Rojas, R. R., Vogeley, M. S., Hoyle, F., & Brinkmann, J. 2004, ApJ, 617, 50

—. 2005, ApJ, 624, 571

Rupke, D. S. N., Veilleux, S., & Baker, A. J. 2008, ApJ, 674, 172

Saintonge, A. 2007, PhD thesis, Cornell University

Salim, S. 2014, Serbian Astronomical Journal, 189, 1

Sánchez Almeida, J., Pérez-Montero, E., Morales-Luis, A. B., et al. 2016, ApJ, 819, 110

Schawinski, K., Urry, C. M., Simmons, B. D., et al. 2014, MNRAS, 440, 889

SDSS Collaboration, Albareti, F. D., Allende Prieto, C., et al. 2016, ArXiv e-prints, arXiv:1608.02013

Shields, G. A., Skillman, E. D., & Kennicutt, Jr., R. C. 1991, ApJ, 371, 82

Stasińska, G., Vale Asari, N., Cid Fernandes, R., et al. 2008, MNRAS, 391, L29

Strateva, I., Željko Ivezić, Knapp, G. R., et al. 2001, AJ, 122, 1861

Strauss, M. A., Weinberg, D. H., Lupton, R. H., et al. 2002, AJ, 124, 1810

Sutter, P. M., Lavaux, G., Wandelt, B. D., et al. 2014, MNRAS, 442, 3127

Thuan, T. X., Izotov, Y. I., & Lipovetsky, V. A. 1995, ApJ, 445, 108

Tonnesen, S., & Cen, R. 2015, ApJ, 812, 104

Tremonti, C. A., Heckman, T. M., Kauffmann, G., et al. 2004, ApJ, 613, 898

van de Weygaert, R., & Platen, E. 2011, IJMPS, 1, 41

van Zee, L., & Haynes, M. P. 2006, ApJ, 636, 214

Vila Costas, M. B., & Edmunds, M. G. 1993, MNRAS, 265, 199

von Benda-Beckmann, A. M., & Müller, V. 2008, MNRAS, 384, 1189

Wilkinson, D. M., Maraston, C., Thomas, D., et al. 2015, MNRAS, 449, 328

Wyder, T. K., Martin, D. C., Schiminovich, D., et al. 2007, ApJSS, 173, 293

Yin, S., Liang, Y., Hammer, F., et al. 2007, A&A, 462, 535

York, D. G., Adelman, J., John E. Anderson, J., et al. 2000, AJ, 120, 1579